

# Characteristics of Magnetorheological Fluids Applied to Prosthesis for Lower Limbs with Active Damping

Oscar Arteaga<sup>1</sup>(✉), Diego Camacho<sup>1</sup>, Segundo M. Espín<sup>2</sup>, Maria I. Erazo<sup>1</sup>, Victor H. Andaluz<sup>1</sup>, M. Mounir Bou-Ali<sup>3</sup>, Joanes Berasategi<sup>3</sup>, Alvaro Velasco<sup>1</sup>, and Erick Mera<sup>1</sup>

<sup>1</sup> Universidad de las Fuerzas Armadas ESPE, Sangolquí, Ecuador  
{obarteaga, docamacho, mierazo, vhandaluz1, apvelasco, epmeral}@espe.edu.ec

<sup>2</sup> Universidad Técnica de Ambato, Ambato, Ecuador  
sespin@uta.edu.ec

<sup>3</sup> MGEP Mondragon Goi Eskola Politeknikoa, Mondragon, Spain  
{mbouali, jberasategui}@mondragon.edu

**Abstract.** The presence of people with amputations makes imminent the necessity of devices that replace the limb in both the aesthetic and functional, for which we propose the design and control of a robotic prosthesis with active damping using Magnetoreological Fluids (MRF) that are a new type of intelligent materials that have been characterized obtaining a shear yield stress of 41,65 kPa applying a controlled magnetic field of 0,8 T with a temperature of 20 °C, in order to have the active damping in the prosthesis will be necessary the use of a Magnetoreological (MR) damper which underwent to a dynamic damping behavior test reflecting 250 N as the maximum damping force. Control with Magnetorheological technology allows to have an instantaneous response in function of the signals obtained from the sensors, so that the patients could have a natural gait.

**Keywords:** Magnetoreological fluids · Robotics · Prosthesis

## 1 Introduction

The diseases, wars, traffic accidents, industrial injuries, and natural disasters, are the main cause of the increase by tens of thousands the number of amputees every year [1], having the body incomplete is not the only inconvenience, considering a sample of 134 people who had a permanent limb loss, 61 of these have used prostheses during the 2 years and almost the half had psychological damages [2]. Due to the current state of medical treatments, limbs cannot regenerate. Therefore, the only way for lower limb amputees to recover the function and appearance of their limbs is to use prosthesis [1], the same ones that have improved and have had significant technological advances in order to improve the quality of life of the patient [3].

Robotics comprises different disciplines in the design of a multidisciplinary system [4], such as a robotic prosthesis which can better restore missing limb functions by

adjusting impedance parameters at different stages of gait and also has the possibility to regulate the dynamic parameters according to the medium field where the patient is using the prosthesis [5].

According to the literature of robotic systems for assistance and rehabilitation, it focusses on providing missing movements and sensing, with environments that are safe and make regaining movement-related function easier and faster. Robotic prosthetics and exoskeletons will provide natural mobility, dexterity and sense of touch to paralyzed or missing limbs [6–8].

It has been possible to minimize the incidence caused by the absence of the lower extremity proposing a robotic prosthetic for lower limbs using MRF whose mechanical properties allows a complete damping control on the walking, the ones that have liquid-like properties without magnetic fields and forms chain-like structures when external magnetic fields are applied [9].

This paper has 5 Sections including the Introduction. The Sect. 2 describes the MRF's properties. The Sect. 3 explain de design of the robotic prosthesis. The Sect. 4 show the experimental results of the MR damper. Finally, the Conclusions are presented in the Sect. 5.

## 2 MRF's Properties

Magnetorheological fluids become a category of magnetically controllable fluids, usually formed by iron particles in a liquid carrier. The basic phenomena that are generated in the magnetoreology are related to the possibility of controlling the structure and, consequently, the rheological behavior of the plastic biphasic fluid through the use of relatively moderate magnetic fields [10].

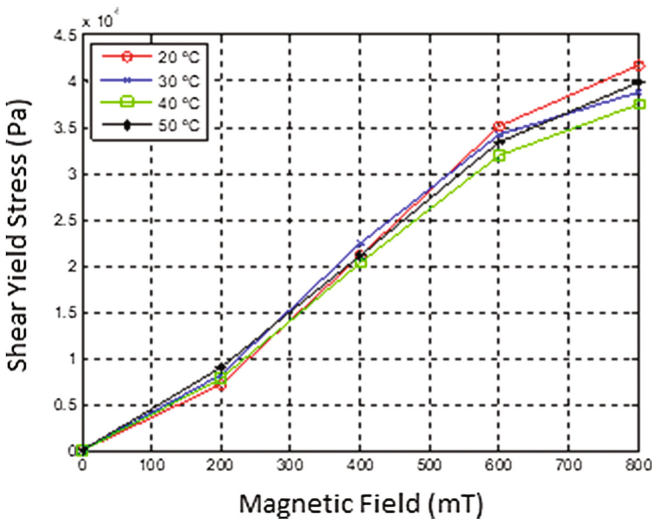


**Fig. 1.** Shear yield stress in function of the magnetic field and temperature.

The employment use of MRF as key components of several high-tech applications involving vibration control or torque transmission, lead to improved performance with new MRF formulations as is the LORD MRF-140CG fluid. Through the magnetic field is controlled the yield stress, shear thinning, and viscosity, that viscoelastic response, are important factors to consider on the MRF [10].

In Fig. 1. is shown the shear yield stress obtained by the MRF characterization at ranges of ranges of different temperatures on 20 °C to 50 °C and magnetic fields of 0 T to 0, 8 T, was performed using the MRC-501 rotational rheometer (Anton Paar Physica) with the MRD-70/1T cell coupled for the application and control of the magnetic field, and for the control of temperature was used a thermostatic Julabo F-25 bath.

### 3 Prosthesis Design

For the patients of 25 to 35 years old of the Percentile 90 [11] presents the anthropomorphic characteristics that are showing on Table 1.

**Table 1.** Parameters of design.

Height [mm]	Weight [kg]
1.700	70

According to Fig. 2. the type of amputation that is taken for the design is a cut of 50[mm] above the knee; taking the standard measures according to the design parameters [11], a knee length up to the ground of 485[mm] is determined and the 50[mm] knee amputees should be taken into account, the appropriate design weight calculated is proportional weights, *i.e.*, 4.15 [Kg].

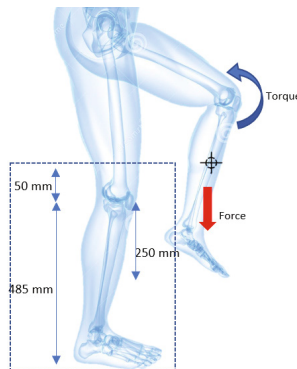


**Fig. 2.** Anthropometric dimensions.

Considering the design parameters and properties of MRF, the transfemoral prosthesis with active damping is designed as shown in Fig. 3.

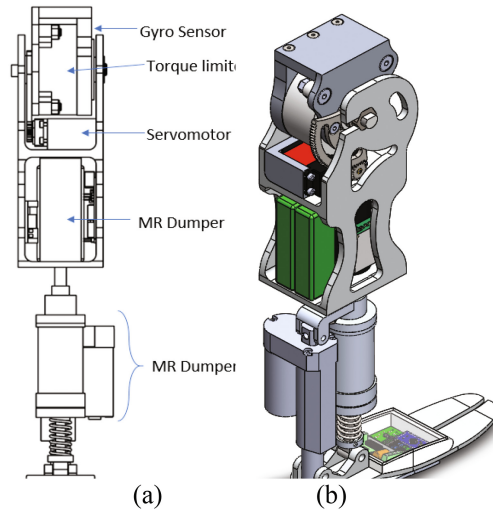


**Fig. 3.** Prosthesis design: (a) the three-dimensional structure and (b) the three-dimensional

Figure 3(a) and (b) respectively show the three-dimensional structure and sectional view of the prosthesis, which was designed and developed according to the principle shown in Fig. 3 [12], the prosthesis is mainly composed by a torque limiter that works as a knee providing the necessary angle for walking, the MR damper that gives enough cushioning acting like normal leg and avoiding several future damages in the other leg.

The DC power supplies are required for the current amplifier, servomotor, MR damper and gyro sensor. The desired knee joint angle ( $\varnothing$ ) and the necessary force require by the MR damper ( $F$ ) are predicted from the hip joint angle which is measured by the gyro sensor. [12] The actual knee joint angle is directly measured by the hall sensor. Therefore, the prosthesis is a closed single input and single output closed-loop system including the nonlinear PD controller as shown in Fig. 4. Therefore, the control input is completely different during the swing phase from that during the stance phase. In the swing phase, control signal input is turned off so that the Torque limiter does not resist the rotation of the servomotor. However, in the stance phase the torque limiter supports the body weight and controls the knee joint angle with force from the servomotor. The force sensor provides the necessary information about the force that changes according to the magnetic flux density ( $B$ ) that MR damper requires to cushion the prosthesis properly.

The transmission of the torque of the torque limiter depends largely on the yield limit and the viscosity of the fluid. The Bingham plastic model is used to describe the behavior of MR in the disk-shaped actuator, [13] and is given by:

$$\tau(r, \omega, H) = \tau_y(H) + \eta \frac{\omega r}{h} \tag{1}$$

Where  $\tau(r, \omega, H)$  is the shear force, which depends on some factors,  $\tau_y(H)$  is the dynamic yield limit that depends on the magnetic flux density,  $\eta$  is the viscosity of the fluid,  $\omega$  is

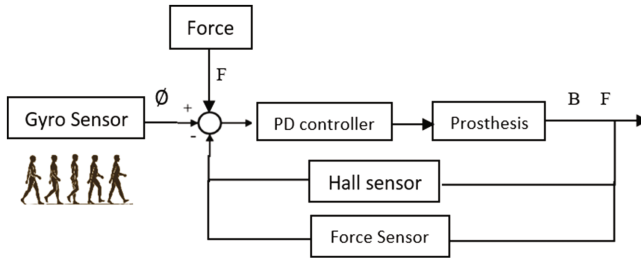


Fig. 4. Block diagram of the prosthesis

the angular velocity of the rotating disk,  $h$  is the fluid interval and  $r$  is the position on the surface of the disk as shown in Fig. 5. The resistive torque can be found derived from the shear off along the surface of the plate [13].

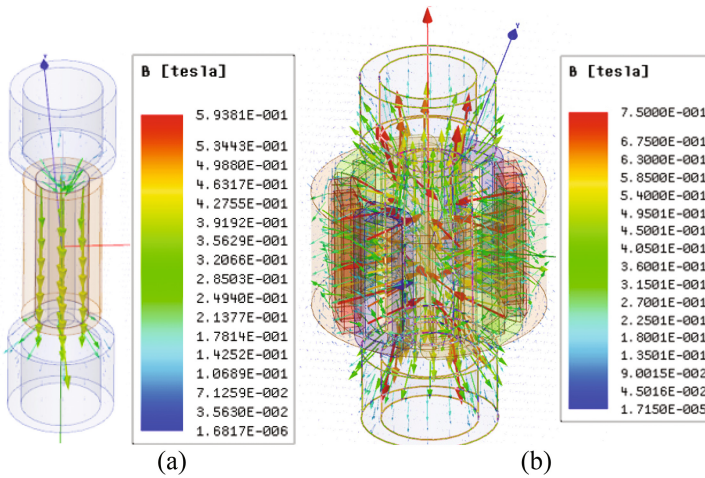


Fig. 5. Magnetic Field analysis: (a) venturi analyzed coil made of 1000 turns with parallel magnetic direction, (b) venturi analyzed with an external coil that produce a perpendicular magnetic direction

$$T = 2 \int_{R_i}^{R_0} (\tau_y(H) 2\pi r) r dr \tag{2}$$

Where  $T$  is the resistive torque,  $R_i$  and  $R_0$  are the inner and outer radius, respectively, substituting Eq. 2 in 1 the torque is given by:

$$T = \frac{4\pi}{3} \tau_y(H) (R_0^3 - R_i^3) + \frac{\eta\omega\pi}{h} (R_0^4 - R_i^4) \tag{3}$$

As can be seen in Eq. 3, the torque consists of two terms: the one is due to the effects of the MRF and the other is due to the viscous flow. The MR torque limiter is designed to

work at very small rotational speeds, so the contribution of viscosity is very small and can be ruled out compared to the effects of the MR so the design is only based on the first term. The MRF used in the actuator is MRF-140CG, supplied by Lord Corporation. The maximum elastic limit in the linear working area is  $\tau_y = 42$  kPa and the corresponding magnetic field is  $H = 100$  kA $m^{-1}$ . The shaft diameter is chosen to be 12.7 mm or  $R_i = 6.35$  mm. As a result, the torque is 4.7 Nm.

On the other hand, for the MR dumper the flow mode consists of a housing, piston, (MRF-140CG), solenoid coil, oil seal, and magnetic core, the magnetic core is made of pure steel for high permeability, and the piston and housing are made of aluminum for low permeability. Thus, the magnetic field, which is generated by the solenoid coil, flows through the magnetic core. According to the Bingham plastic model of plates, the damping force,  $F_D$  is divided into the induced yield stress  $F_\tau$  and viscous components  $F_\eta$ . The damping force is written as follows [12].

$$F_D = F_\tau + F_\eta \quad (4)$$

According to the plate model of Bingham plastic model, the damping force,  $F_D$ , can be divided into an induced yield stress  $F_\tau$  and viscous  $F_\eta$  component.

## 4 Magnetic Field Analysis

The Fig. 5. proves the theory of magnetism, the item (a) shows the flux density parallel to the fluid, where it is not enough to generates the required force in the item (b) the flux density is perpendicular to the fluid resulting in the magnetism necessary to produce the required force for cushioning.

The damping force for the FEM modeling is calculated using the magnetic flux density as determined at different current levels. The yield shear stress  $\tau_y$  relationship with the magnetic flux density (B) for MR fluid MRF-140 EG. For the magnetic flux densities computed in the previous section, the corresponding yield shear stress is found by the rheometer analysis [12].

$$F_d = F_\eta + F_\tau = A_p \left( \frac{12\eta l_p Q}{d_i \pi d_o^3} + c \frac{l_m}{d_o} \tau_y \right) \text{sign}(v), \quad (5)$$

Where,

$$Q = A_p |v| \quad (6)$$

In the above, Q is the volumetric flow rate of the MRF,  $A_p$  is the effective cross-sectional area of the piston,  $d_o$  is the inner diameter of the housing,  $d_i$  is the diameter of magnetic core,  $d$  is the diameter of the piston rod,  $v$  is the piston velocity,  $\tau_y$  is the yield stress of the MRF,  $\eta$  is the offstate no magnetic field viscosity of the MRF,  $l_m$  is the effective axial pole length,  $l_p$  is the annular duct length, and  $\text{sign}(v)$  is used to consider the semi-active force. In order to analyze the magnetic field between the yield stress of the MRF and

input current the finite element method is used, it is analyzed in a CAE software that display the intensity and direction of the magnetic field [12].

### 5 Experiments and Results

In order to bring about an effective MR dumper, the coil is made for producing the necessary magnetic camp to cushion the prosthesis, Fig. 6. the red perpendicular arrows show the principle of keeping the majority of the field in the rod developing a comfortable cushion during the walking, while the torque limiter produce the effective angle to generate a correct movement of the prosthesis.

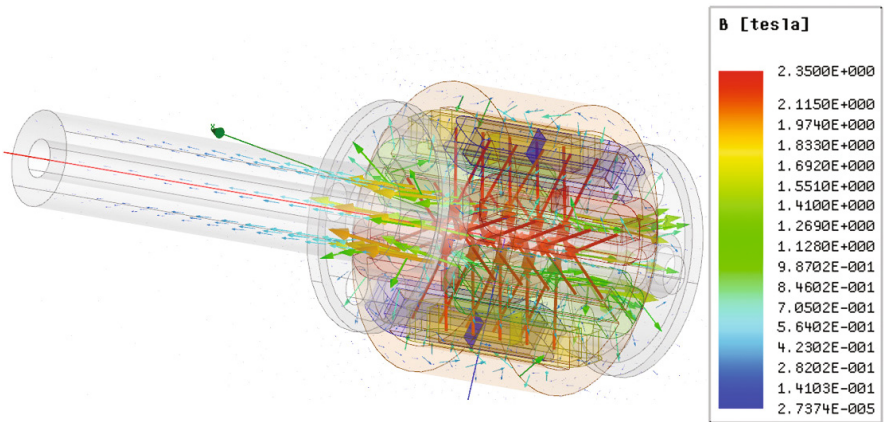


Fig. 6. Piston rod with a perpendicular flux density

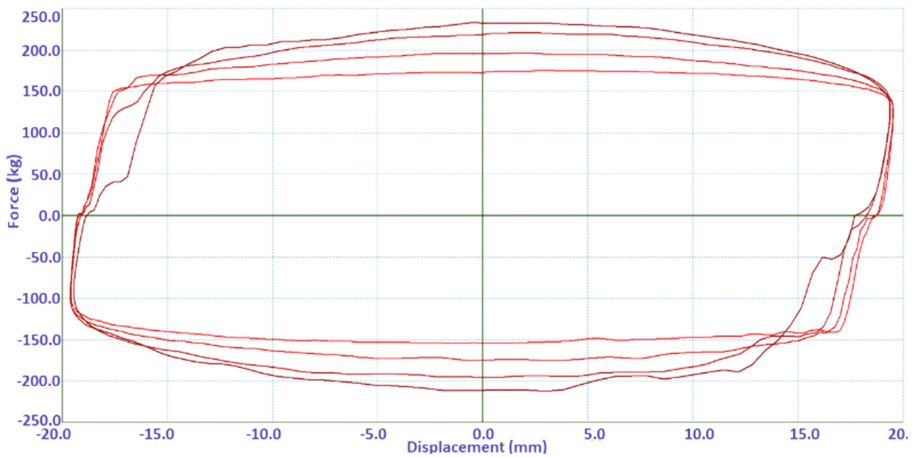


Fig. 7. Force vs Displacement

The test made on the bench Dyno-shock 11, indicates that the damping force is nonlinearly increased by increasing flux density. Figure 7 shows the displacement of the piston versus damping force. The maximum damping force is approximately 250 N. It is remarked here that in this work the MR damper is designed with a high viscosity term depending on the angular velocity of the knee joint angle because the bending angular velocity is fast when the person falls down while walking.

## 6 Conclusions

The control of the prosthesis was done in such way that the patient has an adequate gait according to the environment in which moves and the activity that performs, providing comfort and autonomy to the patient.

The effectiveness of the robotic prosthesis is demonstrated experimentally, obtaining the active damping, a MR damper was used in which its field-dependent characteristics of the MR damper were measured, such as the damping force where it can be seen that to generate an optimal damping is necessary for the walk the induction of a smaller magnetic field and for running requires a high field.

## References

1. Xu, L., Wang, D.H., Fu, O., Yuan, G., Hu, L.Z.: A novel four-bar linkage prosthetic knee based on magnetorheological effect: principle, structure, simulation and control. *Smart Mater. Struct.* **25**, 12 (2016). doi:[10.1088/0964-1726/25/11/115007](https://doi.org/10.1088/0964-1726/25/11/115007)
2. Price, P.: The diabetic foot: quality of life. *Clin. Infect. Dis.* **39**, S129–S131 (2004). doi:[10.1086/383274](https://doi.org/10.1086/383274)
3. Young, A.J., Simon, A.M., Fey, N.P., Hargrove, L.J.: Intent recognition in a powered lower limb prosthesis using time history information. *Ann. Biomed. Eng.* **42**(3), 631–641 (2014). doi:[10.1007/s10439-013-0909-0](https://doi.org/10.1007/s10439-013-0909-0)
4. Ragusilaa, V., Emami, M.R.: Mechatronics by analogy and application to legged locomotion, *Mechatronics. Inf. Process* **000**, 1–19 (2016). doi:[10.1016/j.mechatronics.2016.02.007](https://doi.org/10.1016/j.mechatronics.2016.02.007)
5. Zheng, E., Wang, Q.: Noncontact capacitive sensing based locomotion transition recognition for amputees with robotic transtibial prostheses. *IEEE Trans. Neural Syst. Rehabil. Eng.* **25**, 161–170 (2016). doi:[10.1109/TNSRE.2016.2529581](https://doi.org/10.1109/TNSRE.2016.2529581)
6. Dellon, B., Matsuoka, Y.: Prosthetics, exoskeletons, and rehabilitation. *IEEE Robot. Autom. Mag.* **14**, 30–34 (2007). doi:[10.1109/MRA.2007.339622](https://doi.org/10.1109/MRA.2007.339622)
7. Lawson, B.E., Mitchell, J., Truex, D., Shultz, A., Ledoux, E., Goldfarb, M.: A robotic leg prosthesis: design, control, and implementation. *IEEE Robot. Autom. Mag.* **21**, 70–81 (2014). doi:[10.1109/MRA.2014.2360303](https://doi.org/10.1109/MRA.2014.2360303)
8. Lawson, B.E., Ledoux, E.D., Goldfarb, M.: A robotic lower limb prosthesis for efficient bicyclin. *IEEE Trans. Rob.* **33**, 432–445 (2017). doi:[10.1109/TRO.2016.2636844](https://doi.org/10.1109/TRO.2016.2636844)
9. Park, J., Yoon, G.H., Kang, J.W., Choi, S.B.: Design and control of a prosthetic leg for above-knee amputees operated in semiactive and active modes. *Smart Mat. Struct.* **25**, 13 (2016). doi:[10.1088/0964-1726/25/8/085009](https://doi.org/10.1088/0964-1726/25/8/085009)
10. Susan-Resiga, D., Vékás, L.: Yield stress and flow behavior of concentrated ferrofluid-based magnetorheological fluids: the influence of composition, pp. 645–653. Springer, Heidelberg (2014)



11. Serrano-Sanchez, J.A., Lera-Navarro, A., Espino-Torón, L.: Physical activity and differences of functional fitness and quality of life in older males. *Revista Internacional de Medicina y Ciencias de la Actividad Física y del Deporte* (2016). doi:[10.1093/gerona/56.suppl\\_2.23](https://doi.org/10.1093/gerona/56.suppl_2.23)
12. Xu, L., Wang, D.H., Fu, Q., Yuan, G., Hu, L.Z.: A novel four-bar linkage prosthetic knee based on magnetorheological effect: principle, structure, simulation and control. *Smart Mater. Struct.* **25**(11), 115007 (2016). doi:[10.1088/1361-665X/aa61f1](https://doi.org/10.1088/1361-665X/aa61f1)
13. Sarkar, C., Hirani, H.: Theoretical and experimental studies on a magnetorheological brake operating under compression plus shear mode. *Smart Mater. Struct.* **22**(11), 115032 (2013). doi:[10.1088/0964-1726/22/11/115032](https://doi.org/10.1088/0964-1726/22/11/115032)